International Journal of Pharmaceutics 390 (2010) 250–259

Contents lists available at ScienceDirect

International Journal of Pharmaceutics

journal homepage: www.elsevier.com/locate/ijpharm

Pharmaceutical Nanotechnology

Investigation of the dynamic process during spray-drying to improve aerodynamic performance of inhalation particles

Kohsaku Kawakami[a,b,*], Chihiro Sumitani[a,c], Yasuo Yoshihashi[c], Etsuo Yonemochi[c], Katsuhide Terada[c]

[a] National Institute for Materials Science, Biomaterials Center, 1-1 Namiki, Tsukuba, Ibaraki 305-0044, Japan
[b] International Center for Materials Nanoarchitectonics, 1-1 Namiki, Tsukuba, Ibaraki 305-0044, Japan
[c] Toho University, Faculty of Pharmaceutical Sciences, 2-2-1 Miyama, Funabashi, Chiba 274-8510, Japan

ARTICLE INFO

Article history:
Received 21 October 2009
Received in revised form 6 January 2010
Accepted 10 February 2010
Available online 17 February 2010

Keywords:
Spray-drying
Inhalation
Surface tension
Particles

ABSTRACT

Particle-tailoring technique requires significant improvement for wide use of pulmonary route for systemic drug delivery. In this study, the spray-dry method was used to prepare particles using maltose as a model component, with focus on interpretation of the dynamic process during the spray-drying. High-speed camera observation proved that the time required for particle formation was assumed to be on the millisecond scale. The surface tension at 10 ms was found to correlate well with both the size of the droplet produced from the spray nozzle and that of the solid particles. The surfactant molecules accumulated spontaneously on the particle surface to improve surface characteristics, including dispersity and hygroscopicity. Addition of polymer molecules made the particle surface rough, which significantly improved particle dispersity. Good correlation was found between the surface roughness and the aerodynamic performance of the particles, which was determined by a cascade impactor. The particle morphology was interpreted in terms of the mass transport of each component during the drying process. This excipient approach seems to be a promising method to prepare fine drug particles of high dispersity for achieving an efficient pulmonary drug delivery.

© 2010 Elsevier B.V. All rights reserved.

1. Introduction

Inhalation therapy has been regarded as a promising method for systemic drug delivery as well as treatment of pulmonary diseases such as asthma. Therefore, the launch of Exubera, the first inhalable formulation for insulin therapy, received great attention. However, it was withdrawn quickly due to marketing problem to reveal that significant improvement was still required for inhalation technology in terms of both devices and formulations.

This paper describes development of formulation technology for inhalation therapy. It is widely recognized that particle size is one of the most important factors in determining the deposition site of the formulation in the lung (Bisgaard et al., 2001; Katz et al., 2001; Hickey, 2006; Patton and Byron, 2007; Shekunov et al., 2007; Glover et al., 2008; Park and Wexler, 2008; Yang et al., 2008). There are several deposition models available. The most famous one is the ICRP (International Commission on Radio Protection) model (Smith, 1994), which was developed by assembling experimental observations with model calculations that considered a complicated lung morphology. According to this model, particles smaller than 100 nm most effectively reach the alveoli region. However, this size of particles is almost impossible to manufacture using current formulation technology. Moreover, even if such a formulation can be developed, it will be difficult to prevent aggregation during storage. Thus, micron-sized particles are regarded as the best option for pulmonary drug delivery, although these particles are not free from the aggregation problem either.

Much effort has focused on overcoming the aggregation problem. The most common approach is the use of a carrier with high dispersity, such as lactose, on which the drug particles are adsorbed. Mixing of lactose particles of a different size is more effective (Zeng et al., 1998; Jones and Price, 2006; Jones et al., 2008; Adi et al., 2007), although the detailed mechanism is still under discussion. Because lactose particles are usually larger than drug particles by one or two orders of magnitude, they cannot reach deep into the lungs. Thus, the drug particles must be detached from the carrier particles during the inhalation process. Precise control of the interaction force between the drug particles and the carrier particles to achieve this "ideal" behavior is difficult. Therefore, it is desirable to provide good dispersity to the drug particles themselves by designing appropriate surface characteristics.

Spray-drying is the most common method used to manufacture inhalation particles, and the dynamic particle-formation process must be understood in order to control particle morphology. The particle size has usually been controlled by varying instrumen-

* Corresponding author at: National Institute for Materials Science, Biomaterials Center, 1-1 Namiki, Tsukuba, Ibaraki 305-0044, Japan.
E-mail address: kawakami.kohsaku@nims.go.jp (K. Kawakami).

0378-5173/$ – see front matter © 2010 Elsevier B.V. All rights reserved.
doi:10.1016/j.ijpharm.2010.02.018

Table 1
Surfactants used in this study.

Surfactants	Abbreviation	Supplier	Molecular weight	HLB	CMC(ST) (μg/ml)	CMC(F) (μg/ml)	Reference for CMC values
Sodium dodecyl sulfate	SDS	Wako Pure Chemicals	288	40	2400	2500	Kawakami et al. (2006)
Polyoxyethylene(9) monolauric ether	C12E9	Nikkol	582	14.5	580[a]	–	–
Polyoxyethylene(20) sorbitan monooleic ester	Tw80	Nacalai Tesque	1300	15	14	15	Kawakami et al. (2006)
Tocopheryl polyethyleneglycol succinate	TPGS	Eastman	1500	13	200[a]	27	–
Gelucire 44/14	Gelucire	Gatte fosse	1900	14	2	2	Kawakami et al. (2004)
Polyoxyethylene(60) hydrogenated castor oil	HCO-60	Nikkol	3600	14	–	98[b]	Priev et al. (2002)

CMC(ST): CMC obtained by the surface tension method and CMC(F): CMC obtained by the fluorescent method.
[a] Information from supplier.
[b] CMC of Cremophor EL.

tal conditions including nozzle diameter and atomizing pressure (Okuyama and Lenggoro, 2003; Chow et al., 2007). Regarding the solution conditions, concentration is known to affect particle size, that is, smaller particles can be obtained by reducing the solution concentration (Okuyama and Lenggoro, 2003; Jones et al., 2008). It is easily assumed that surface tension should affect particle size. However, no clear correlation has been presented on this because discussions have frequently been made using equilibrium surface tensions, which are not likely to be obtained in the spray-drying process. In addition to the control of the particle size, there are many other ways to improve the aerodynamic behavior of the inhalation formulation. The most representative approach is to prepare low-density particles including hollow (Tsapis et al., 2002; Hadinoto et al., 2007) or porous (Edwards et al., 1997; Yang et al., 2009) particles, because this leads to a decrease in aerodynamic size. Surface characteristics including surface roughness (Chew et al., 2005) and surface energy (Tong et al., 2006) are also important for controlling the dispersity of the particles. In this paper, the dynamic process during spray-drying is discussed to explain the morphology of the dried particles. The strategy to obtain particles suitable for pulmonary drug delivery, in which excipients were used to improve the aerodynamic behavior, is also discussed.

2. Experimental

2.1. Materials

The surfactants used in this study are summarized in Table 1. Maltose, lactose, bovine serum albumin (BSA), poly(vinyl pyrrolidone) (PVP) k90 and methylcellulose (MC) were obtained from Nacalai Tesque (Kyoto, Japan). L-Serine, L-threonine, and L-glutamic acid were purchased from Wako Pure Chemicals (Osaka, Japan). All the sugars and the amino acids were of the guaranteed reagent grade with purity higher than 99%, while all the polymers are of the extra pure or the general reagent grade. Exact purity values for the polymers and the surfactants were not available except for BSA and SDS, of which the purity was higher than 98%. All the reagents were used as supplied.

2.2. Dynamic surface tension

Dynamic surface tension of the feed solution in the millisecond time scale was measured on BPA-800P surface tensiometer (KSV Instruments, Helsinki, Finland) at ambient temperature. A capillary with a diameter of 0.13 mm was rinsed by distilled water, ethanol, and acetone before measurements, followed by calibration using distilled water. About 30 ml of the solution was subjected to measurements. The immersion depth of the capillary was 5 mm. Each measurement was repeated at least twice to confirm reproducibility.

2.3. Spray-drying

Spray-drying was performed on Ohkawara DL-41 (Ohkawara Kakohki, Yokohama, Japan) with the following operational conditions: inlet temperature 210 °C, feeding rate of the solution 7 ml/min, and maltose concentration 9.5 wt%. The solution was sprayed from a nozzle with a 0.7 mm diameter with a nitrogen flow of 0.2 MPa atomizing pressure. The viscosity of the solution was measured using a Ubbelohde viscometer to prove that viscosity of all the feed solutions was identical at 1.1 mPa s except the polymer solutions. The outlet temperature was about 90–95 °C in all cases. More than two lots of the samples were prepared for each composition.

2.4. Observation of the spray with a high-speed camera

The sprayed droplets from the nozzle were observed using a high-speed video camera HyperVision HPV-2 (Shimadzu, Kyoto, Japan) in which a million images were captured per second. Because the focus distance was a few centimeters, observations were only possible without the drying chamber. Thus, the observation was made under ambient temperature and pressure conditions. The velocity of the droplets was determined from images obtained both 0.5 and 3 cm below the nozzle.

2.5. Droplet size measurement

The surfactant solutions were sprayed using a spray-dry nozzle under ambient pressure and temperature conditions identical to those during high-speed video camera observation. The droplet size 3 cm below the nozzle was determined by a laser diffraction method on Nikkiso Aerotrac SPR (Nikkiso, Tokyo, Japan). The distance from the laser source to the droplets was about 5 cm. Measurements were repeated at least three times to obtain mean values, of which the standard deviations were always smaller than 10%.

2.6. Scanning electron microscopy (SEM)

The SEM images of the particles were obtained on JSM-5600 (JEOL, Tokyo, Japan). Particles were loaded on the sample stage in a dry bag, in which the humidity was maintained below 20%RH. Platinum coating with an estimated thickness of 50 nm was per-

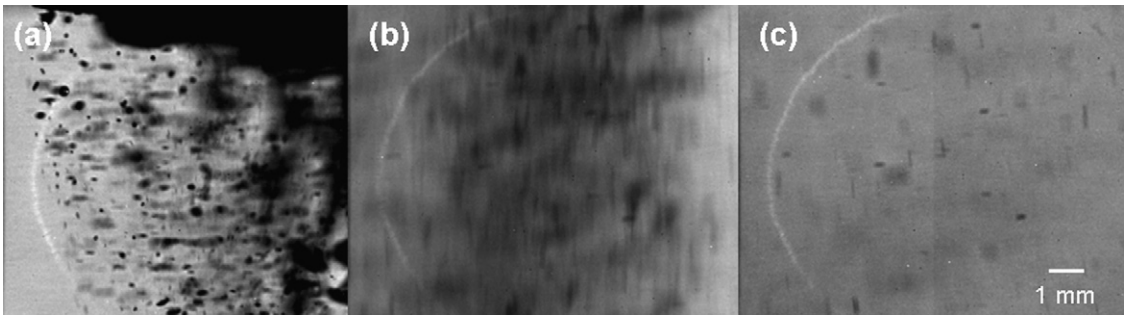

Fig. 1. Snapshots of the atomizing process by a high-speed camera. 4%SDS aqueous solution was sprayed under ambient temperature and pressure. (a) Just below the nozzle. Droplets moving downward were too fast for the detection. The large droplets in the figure were moving upward slowly. (b) 5 mm below the nozzle. All droplets were moving downward. (c) 3 cm below the nozzle. All droplets were moving downward. Because the droplets were scattered, the camera could only focus on a small fraction of droplets.

formed on ESC-101 (Elionix, Tokyo, Japan). The accelerating voltage for measurements was 20 kV.

2.7. Particle size measurement

The size of the particles was determined by image analysis of the SEM pictures using Mac-View ver.4 (Mountech, Tokyo, Japan). Three hundred particles were selected randomly from the image to obtain the Heywood diameter. Volume-mean diameter was used for the analysis except when calculating the theoretical surface area where area-mean diameter was used.

2.8. Assessment of surface composition by X-ray photoelectron spectroscopy (XPS)

Surface composition of the particles was determined by XPS (AXIS-NOVA, Kratos Analytical, Manchester, UK), during which a surface layer of about 5 nm was analyzed. The surface concentration of carbon and oxygen atoms was assessed to convert their ratio to the molecular ratio of the components. For example, C:O ratio of maltose was 12:11, while that of TPGS was 77:27. Such significant difference in the C:O ratio enabled determination of the maltose:TPGS ratio on surface. When SDS was used as a surfactant, the surface concentration of a sulfur atom was analyzed to obtain the surface concentration of SDS. Nitrogen atoms were investigated for quantification of amino acids or BSA.

2.9. Hygroscopicity

Hygroscopicity of the particles was evaluated on a Dynamic Vapor Sorption analyzer (Surface Measurement Systems, Middlesex, UK). About 3 mg of the sample was loaded on a cell, followed by exposure to dried air at 50 °C for about 2 h. After confirming that the baseline is stable at 25 °C, the relative humidity was changed to 20%. The amount of the water adsorbed was determined after 2-h equilibration. This humidity was selected to obtain reproducible values, because exposure of powders at higher humidity resulted in formation of plasticized layers on the surface that inhibited access of vapor to inner regions of the powder. The measurement at higher humidity had problem in the quantitative reproducibility, however, trend of the result was coincident with that of 20%RH. Thus, improvement in the hygroscopic behavior at ambient conditions seemed to be estimated form the assessment at 20%RH.

2.10. Surface area

Surface area of the powders was determined by the nitrogen adsorption method on Belsorp mini (Bel Japan, Osaka, Japan). The samples were dried at 50 °C for 30 min under vacuum prior to measurement. About 100 mg of samples were subjected to measurement. Each measurement was repeated twice to obtain the mean surface area calculated by the BET method.

2.11. Cascade impactor

Non-viable eight-stage Cascade Impactor AN-200 (Tokyo Dylec, Tokyo, Japan) was employed to determine the fraction of fine particles. About 100 mg of the powder was loaded in a Diskhaler, followed by administration for 5 s at an air flow rate of 28.3 L/min. A small amount of liquid paraffin was loaded on the collector to trap the particles. The trapped amount was evaluated by weight. The particles collected during stages 2–8 were defined as the fine particles, of which the hydrodynamic diameter was assumed to be below 7 μm.

2.12. Other powder characteristics

All samples prepared were confirmed to be in the amorphous state when maltose was used as a main component and in the crystalline state (form γ) when lactose was used as a main component, using the X-ray diffraction method (Rint-Ultima III, Rigaku, Tokyo, Japan). Density was measured using 5-ml pycnometers, for which ethanol was used as a solvent.

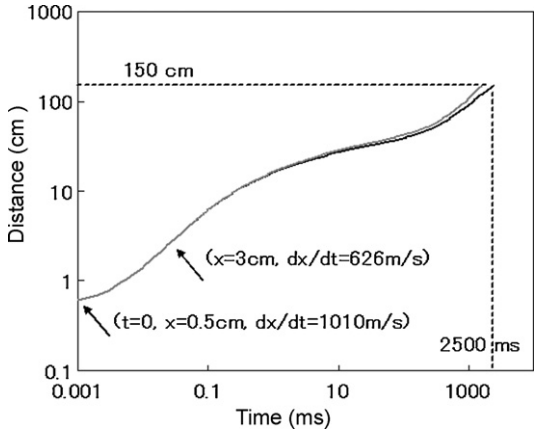

Fig. 2. Relationship between the distance of droplets from the spray nozzle and time calculated by Eq. (1) numerically. The black line was obtained by ignoring the decrease in the droplet size due to the evaporation. The gray line was calculated assuming a constant decrease in droplet volume. The boundary conditions obtained by observations using a high-speed camera are presented in the figure.

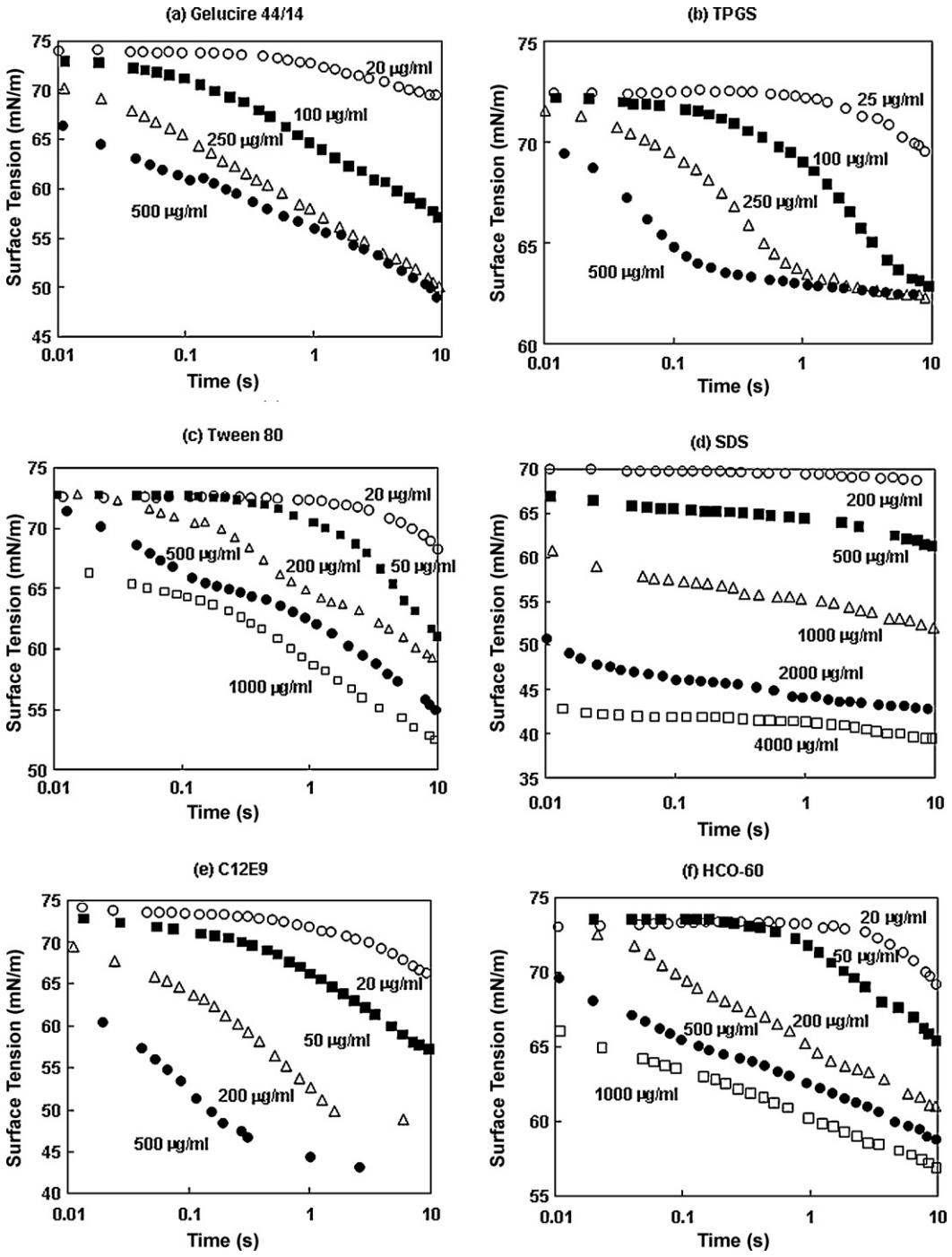

Fig. 3. Dynamic surface tension of aqueous surfactant solutions at room temperature. The surfactant type and the concentration are shown in the figure. Each measurement was repeated at least twice to provide representative data. CMC of each surfactant is available in Table 1.

3. Results and discussion

3.1. Investigation of the atomization process

To understand the dynamic process during formation of particles, the atomizing process was investigated using a high-speed video camera. Fig. 1 visualizes the atomization process of surfactant solutions. The feeding rate of the solution, nozzle diameter, and viscosity of the solution resulted in a Reynolds number greater than 100,000, meaning that a laminar flow was not expected. The atomized droplets did not fall only in the vertical direction but also moved in other directions including upward, suggesting that collision could occur after atomization. Observation at a few centimeters below the atomization nozzle revealed that the flow of the droplets was more homogeneous. The diameter of the droplets was around 10 μm; however, large droplets (almost millimeter scale) were occasionally found. These observations suggest the existence of difficulties in the theoretical prediction of the size of the atomized droplets.

Analysis of images of the atomization process provided a mean velocity of droplets as ca. 1010 m/s at 5 mm and ca. 626 m/s at 3 cm below the nozzle. The falling distance of the droplets, x, as a function

of time, t, may be understood using the equation of motion shown below.

$$m\frac{d^2x}{dt^2} = mg - k\left(\frac{dx}{dt}\right)^2 \quad (1)$$

Here m and k are the weight of each droplet and the friction coefficient, respectively. g is the acceleration of gravity. This equation was numerically solved assuming m was either a constant or monotonically decreasing function with time (Fig. 2). Although determination of the shrinkage speed of the droplets is outside the focus of this paper, the calculation results suggest that the decrease in the droplet volume has only a small impact. The length of the drying chamber of the spray-dryer was about 1.5 m. The calculation results provide a residence time of the droplets/particles in the chamber of 2.5 s under the assumption of the constant m, which should be a slight overestimation because of actual decrease in m with time. This calculation indicates that the spray-drying process can be completed within a few seconds, which is in agreement with the generally accepted residence time of this process. Thus, it is obvious that the dynamic process in the millisecond time scale needs to be comprehended to control the particle-formation process.

3.2. Dynamic surface tension of surfactant solutions

The surface tension of the feed solutions is expected as one of the most important factors to determine the size of the spray-dried particles. Although some literature has already indicated a possible correlation between them, no clear relationship has thus far been presented. One problem on this kind of discussion is that the equilibrium surface tension has been employed for the evaluation. However, it is obvious that the equilibrium surface tension cannot be obtained during the spray-dry process, because particle formation is completed within a few seconds, as revealed by the model calculation. Thus, the surface tension in a millisecond time scale was evaluated for solutions used in this study.

Fig. 3 shows the dynamic surface tensions of the surfactant solutions. The equilibrium surface tension was not obtained even above the critical micellar concentration (CMC) in this time scale, except for SDS. This result clearly suggests that the equilibrium "low" surface tension cannot be expected during the spray-drying process, even if the surfactants were added at a concentration higher than the CMC. The surface activation process can be divided into three steps: (1) diffusion from bulk to the surface, (2) adsorption onto the surface, and (3) orientation of the molecules at the surface, which is notably important for high molecular weight compounds. If the process is diffusion-controlled, the following equation can be obtained (Chang and Franses, 1995):

$$\gamma_0 - \gamma = 2RTC\left(\frac{D_{app}}{\pi}\right)^{0.5} t^{0.5}, \quad (2)$$

where γ_0 and γ are the surface tensions of solvent and solution. C and D_{app} are concentration and apparent diffusion coefficient, respectively, and R and T have their usual meanings. According to this equation, $(\gamma_0 - \gamma)/C$ must be proportional to the square root of time if the surface activation is diffusion-controlled. Fig. 4 shows the relationship between $(\gamma_0 - \gamma)/C$ and the square of time of TPGS. The proportional relationship was observed in the initial time period. With an increase in the concentration, the proportional region narrowed and the slope of the fitting line steepened. The same trend was observed for all the surfactants except SDS. Table 2 shows the diffusion coefficients of each surfactant obtained from the slope of the fitting line. General trend was that the diffusion coefficient increased with the increase in the concentration to reach a constant value. These diffusion coefficients were of typical values of nonionic surfactants (Chang and Franses, 1995). However, those

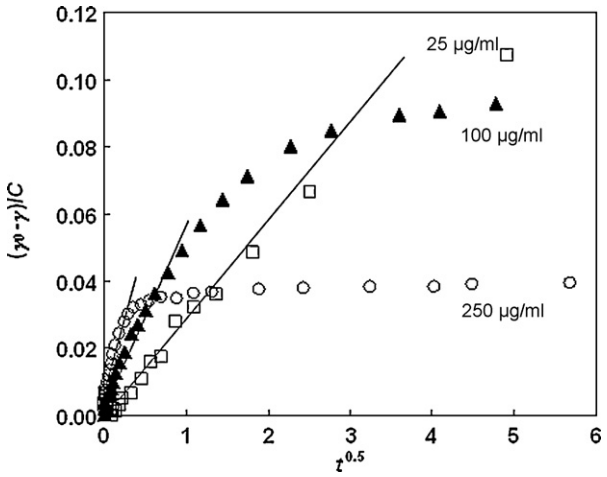

Fig. 4. Relationship between $(\gamma_0 - \gamma)/C$ and square of time for TPGS with linear fittings in the short time range. The concentration is shown in the figure.

of Gelucire and HCO-60 were higher than those of other surfactants by an order of magnitude, which might be due to the presence of a relatively high level of impurities (unreacted species). Although the molecular weight and the CMC can be expected to affect the diffusion coefficient, no clear dependence on those factors was observed for these surfactants. As for SDS, because the decrease in the surface tension was quick, analysis according to Eq. (2) was not possible. The quick decrease in surface tension can be elucidated in terms of the high CMC, meaning that the monomer concentration in the bulk phase is high. Therefore, many SDS molecules are expected to already exist near the droplet surfaces when new surfaces are created, that is, mean diffusion length to the surface can be regarded as short. Another contribution may be from the low molecular weight of SDS, which is inversely proportional to the diffusion constant. However, because C12E9, which also has a small molecular weight, exhibited similar decay curves with other nonionic surfactants, its contribution should be marginal.

3.3. Effect of surface tension on droplet diameter

Fig. 5 shows the correlation between the droplet diameter and the surface tension. The diameter values were consistent with those from the visual observation using high-speed video camera. The

Table 2
Apparent diffusion coefficients (D_{app}) of surfactants.

Surfactants	Concentration (μg/ml)	$D_{app} \times 10^{10}$ (m²/s)
TPGS	25	1.65 (0.53)
	100	6.33 (1.52)
	250	6.10 (0.36)
Gelucire	20	8.50 (3.49)
	50	55.0 (9.5)
	250	45.7 (8.2)
Tw80	20	3.78 (3.56)
	50	1.42 (0.49)
	200	8.51 (4.12)
	250	6.00 (0.34)
C12E9	20	7.37 (0.47)
	50	9.02 (0.17)
	100	9.77 (1.90)
	200	7.70 (1.40)
HCO-60	20	10.2 (8.7)
	50	37.1 (19.1)
	200	117 (12)

Values in parentheses are standard deviations.

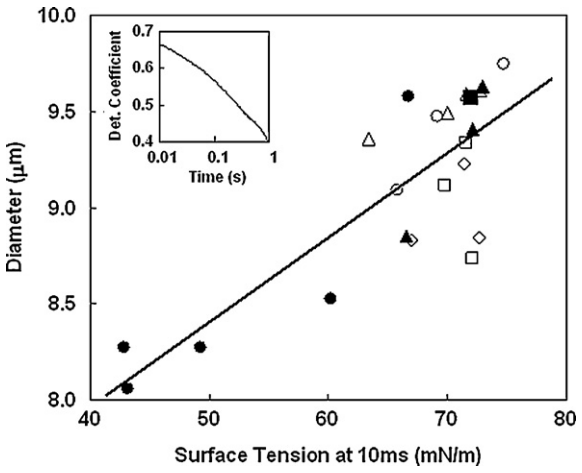

Fig. 5. Dependence of droplet diameter produced from the spray nozzle on surface tension of the feed solution at 10 ms. The surfactants used were SDS (●), HCO-60 (○), TPGS (□), Gelucire (▲), C12E9 (△), and Tw80 (◊). Water (no surfactants) is expressed as ■. Inset shows the determination coefficient as a function of the representative time point to extract the surface tension value.

question remains as to which time point should be selected to obtain the representative surface tension value for evaluation. Inset shows the effect of the time point selected on the goodness of fit. The correlation improved as time decreased. Although the time required for the spray-drying process was determined as within a few seconds, the droplet formation had obviously been completed at the very early stage in the process. The improvement in the goodness of the fit with the decrease in time may suggest that the atomization was a quicker process than 10 ms. Due to the experimental limitation, the surface tension at 10 ms was used for the investigation of the relationship between the surface tension and the droplet size.

It is clearly seen that the correlation was good regardless of the surfactant type, suggesting that the surface tension in the millisecond time scale could be regarded as the dominant factor to determine droplet size. It should be noted, however, that viscosity may also be an important factor in determining droplet size. In this study, the solution viscosity was constant at 1.1 mPa s, and thus further investigation may become required if high-viscosity solutions are used.

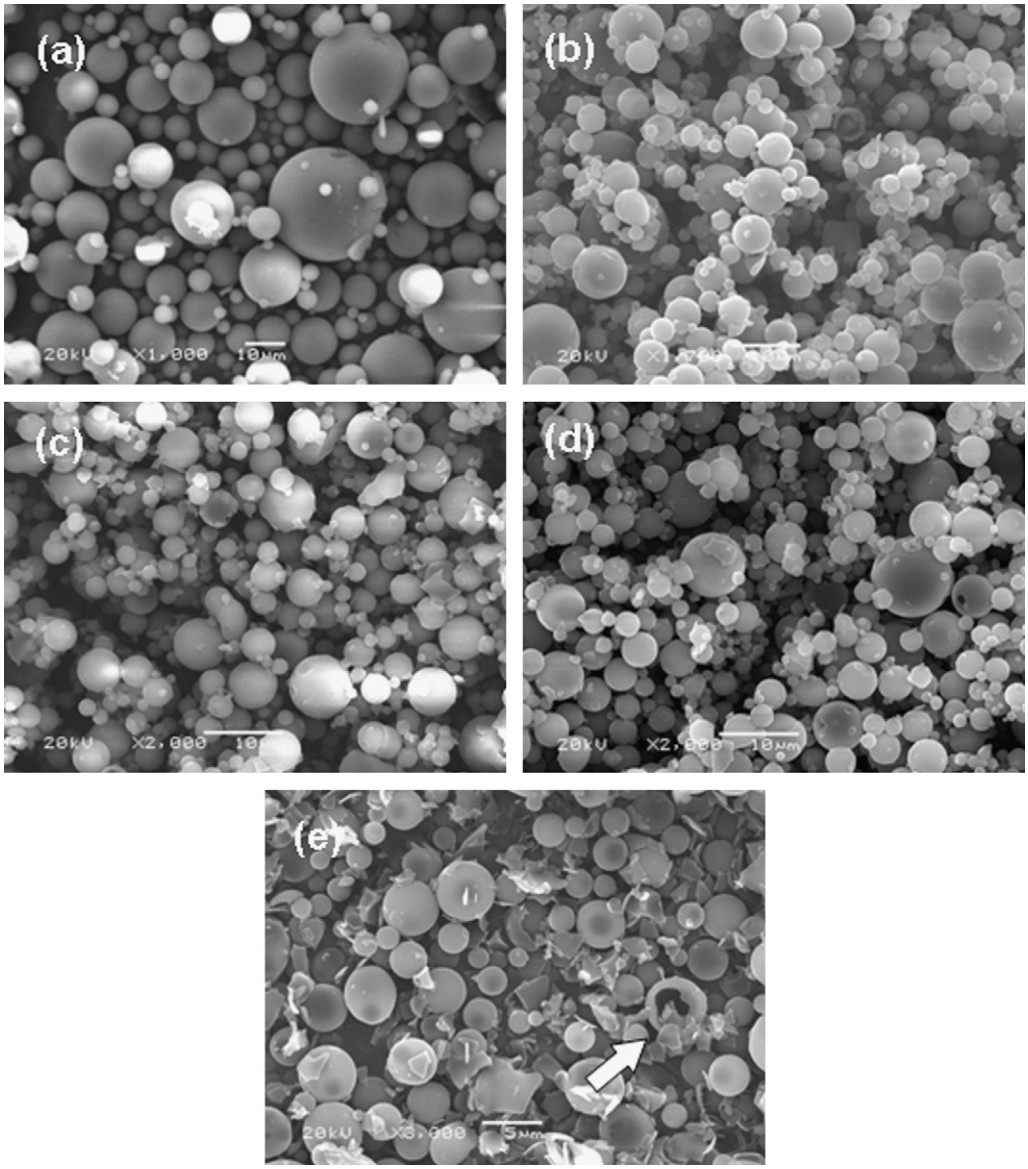

Fig. 6. SEM images of spray-dried particles. (a) Maltose, (b) maltose + 0.5%Gelucire, (c) maltose + 0.5%TPGS, (d) maltose + 0.5%Tw80, (e) maltose + 4%SDS. The arrow in (e) indicates the presence of the hollow particle.

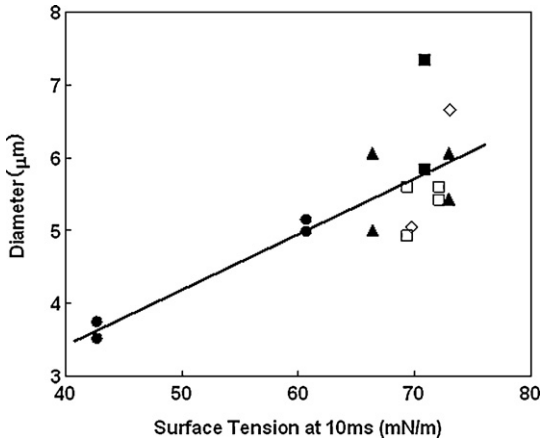

Fig. 7. Dependence of the diameter of the spray-dried particles on the surface tension of the feed solution at 10 ms. Symbols are the same as those for Fig. 5.

3.4. Morphology of spray-dried particles

SEM investigation was performed for spray-dried maltose particles with or without surfactants to prove that all particles obtained in this study were spherical (Fig. 6). When 4% of SDS was added, hollow particles could be found with many fragments that were most likely due to bursting of particles. The formation of the hollow structure can be explained by considering mass transport of each component to the radial direction during the drying process (Vehring, 2007; Vehring et al., 2007). Peclet number, *Pe*, is a convenient measure to discuss this process.

$$Pe = \frac{R_d^2}{\tau D_i} \tag{3}$$

where R_d, τ, D_i are the radius of the droplet, the drying time, and the diffusion coefficient of the component *i*, respectively. A large *Pe* means that the component cannot follow the shrinkage of the droplets, and thus the component is likely to accumulate on the surface region. If this is the case for all components included, then hollow particles are expected. On the other hand, a small *Pe* means that the diffusion of the component is sufficiently fast to follow the shrinkage of the droplets. In this case, homogeneous distribution of the component in the particle is expected. Because D_i of the main component, maltose, is equal for all particles, and the difference in R_d was only marginal, the only possible factor to alter *Pe* dramatically is the difference in the drying time. Formation of a surfactant layer on the air/liquid interface has been pointed out to affect heat transfer of the solution (Wu et al., 1998; Zhang and Wang, 2003). Therefore, the hollow structure obtained by the addition of SDS may be elucidated in terms of the increase in evaporation rate, that is, the decrease in the drying time.

Fig. 7 shows the particle size as a function of the surface tension of the feed solution at 10 ms. The correlation between particle size and surface tension was not as good as it was for the droplets, although the figure suggests that surface tension is still an important factor to determine particle size. Given that one particle was formed from one droplet, the diameter of the particle, D_p, can be calculated by using the diameter of the droplet, D_d.

$$D_p = D_d \left(\frac{\rho_d}{\rho_p} C \right)^{1/3} \tag{4}$$

where ρ_d and ρ_p are densities of the droplet and the particle, respectively. ρ_d is almost unity at ambient temperature. *C* is fraction of the solute in the droplet, that is, the concentration (w/w). The effect of the surfactants on the particle density will be discussed later, but the values obtained are available in Table 3. Using these values, the diameter of the maltose particles with 4%SDS is calculated as 3.6 μm, which is in good agreement with the observation. However, this is not the case for other particles. For example, the diameter for 0.5%TPGS particles was expected to be 3.7 μm, although the actual size was 5.3 μm, indicating fusion of the droplets and/or particles during the spray-drying process. Also should be noted is that the typical spray-dryer, including the setup used in this study, cannot capture very small particles, because they are collected using a cyclone. Nevertheless, the surface tension in the millisecond time scale may be useful as a guide for controlling particle size.

3.5. Surface composition

In addition to the particle size, surface characteristic of the particles is an important factor to be controlled to achieve efficient pulmonary drug delivery. An XPS study was performed to determine the ratio of carbon and oxygen atoms at the surface region, from which the ratio of maltose and surfactants was calculated. When SDS was used as the surfactant, the amount of SDS molecules was determined from the proportion of sulfur atoms exposed on the surface. The weight percentage of the surfactant molecules exposed on the surface is presented in Table 3. In the cases of Gelucire and TPGS, 89.6% and 81.8%, respectively, of the surface was occupied by surfactant molecules by the addition of only a trace amount, 0.5%. The coverage by SDS was modest, most likely due to its high CMC, that is, its relatively high concentration in the bulk phase.

The mechanism of this surface accumulation can be elucidated in terms of the surface active characteristics of the surfactant molecules. In addition, it has been suggested that solubility differences might cause such surface accumulation (Vehring et al., 2007), because a low solubility component may be preferentially crushed out to remain in the surface area during the drying and shrinking process. To confirm this possibility, three types of amino acids with different solubility were used as additives for particle formation, and the degree of the surface accumulation was compared. The amino acids used were L-serine, L-threonine, and L-glutamic acid, of which an aqueous solubility was ca. 330, 100, and 7.4 g/L, respectively. It should be noticed that the solubility of maltose is almost equal with that of L-serine. 9.5%maltose/0.3%amino acid aqueous solutions were spray-dried to find that the percentage of the surface coverage of each amino acid was 2.0, 3.4, and 2.6%, respectively, meaning that the surface component ratio agreed with that of the bulk in all cases. Even though the solubility difference between serine and glutamic acid was more than an order of magnitude, no difference in the accumulation tendency was observed. Therefore, the solubility difference was not confirmed as a driver for the surface accumulation at least in our experimental condition.

Table 3
Characteristics of spray-dried particles.

Additive	Surfactant on surface (%)	Density (g/cm^3)	Surface area (m^2/g)	Water adsorption (g/m^2)	DSI
None	–	1.55 ± 0.02	0.53 ± 0.00	6.11 ± 2.85	0.70
4% SDS	28.2 ± 4.2	1.19 ± 0.02	1.66 ± 0.01	2.10 ± 0.22	1.06
0.5% Tw80	55.9 ± 20.1	1.46 ± 0.04	0.55 ± 0.03	6.42 ± 0.63	0.61
0.5% TPGS	81.8 ± 7.6	1.44 ± 0.09	0.61 ± 0.14	2.04 ± 0.97	0.73
0.5% Gelucire	89.6 ± 5.8	1.41 ± 0.07	1.19 ± 0.09	2.84 ± 0.97	1.04

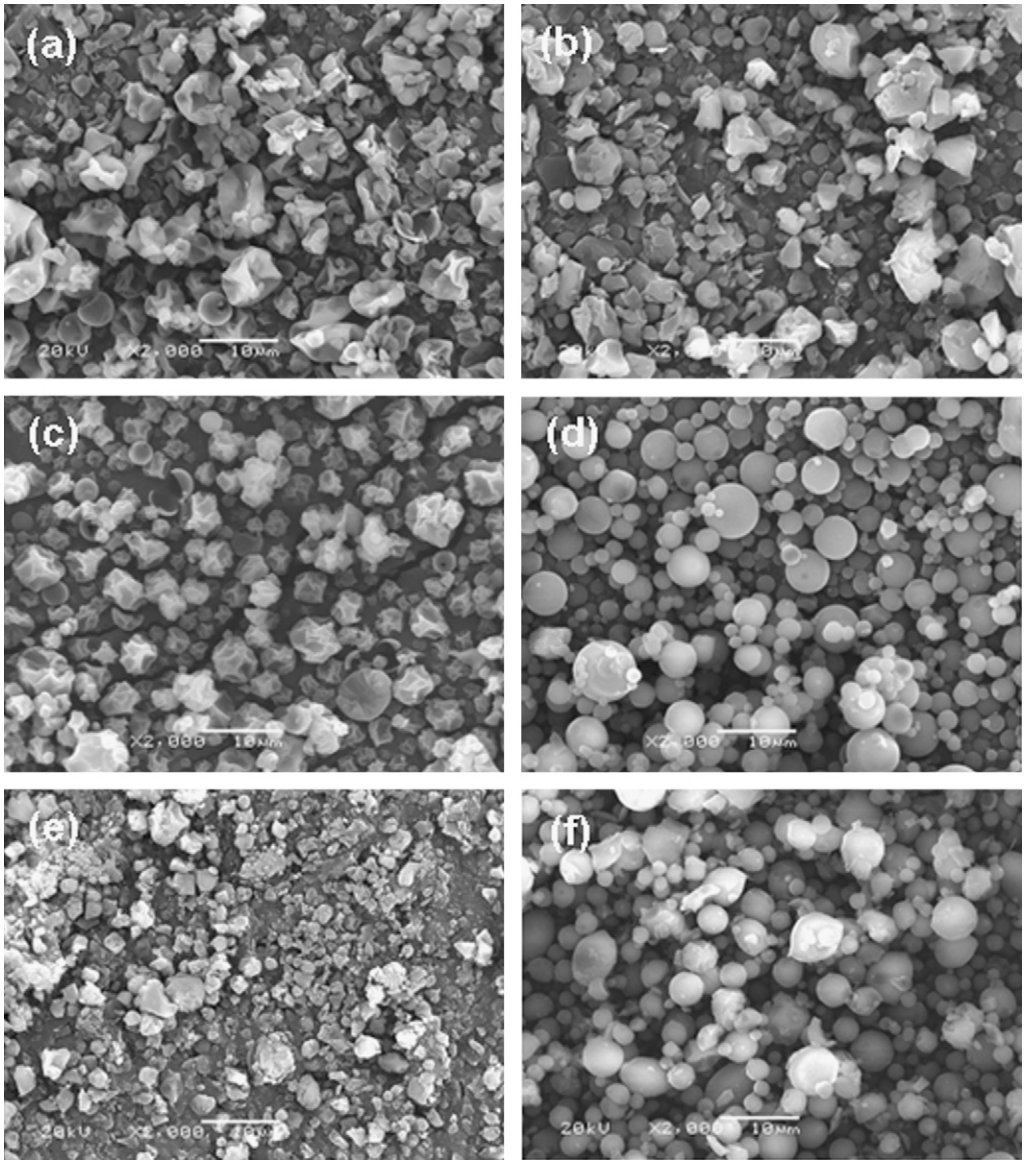

Fig. 8. SEM images of the spray-dried particles. (a) Maltose + 4%MC, (b) maltose + 4%MC + 0.5%Gelucire, (c) maltose + 5%BSA, (d) maltose + 5%BSA + 0.5%Gelucire, (e) mannitol + 4%MC, and (f) mannitol + 10%BSA.

Supersaturation may easily be maintained during particle formation because of the quickness of the spray-drying process.

3.6. Surface area, density, and hygroscopicity

Table 3 also shows the other powder characteristics of the spray-dried particles. The density of the maltose particle exhibited typical values for spray-dried carbohydrates, suggesting that the particle seemed to have a homogeneous (i.e., not hollow) structure. It decreased with the addition of surfactants, notably SDS, which was most likely due to the formation of the hollow structure. These observations are favorable for designing inhalable particles, because a decrease in the hydrodynamic radius contributes to deep deposition of particles in the lung.

Hygroscopicity is an important factor to be controlled, because adsorption of water on the surface enhances adhesion force between the particles. The addition of surfactant molecules decreased hygroscopicity, although the added amount was small, which was most likely due to the preferential accumulation of surfactants onto the surface. Since the surfactant molecules are usually aligned on the air/water interface with their hydrophobic tails directed gas phase, the most outer surface of the resultant particles are likely to be covered by the hydrophobic tails. Therefore, the addition of a small amount of surfactant seemed to be effective at controlling the surface characteristics of the spray-dried particles.

The surface area increased with the addition of the surfactants except with Tw80. When Tw80 was added, the powder became sticky. Therefore, the apparent decrease in the surface area was most likely due to the strong aggregation of the particles. The increase in the surface area by the addition of other surfactants, notably by SDS and Gelucire, can be elucidated in terms of the decrease in the particle diameter and improvement in the dispersity.

The experimental surface area was divided by the theoretical surface area, which was calculated from the SEM images by using area-mean particle size and assuming a spherical shape, to obtain dispersity/surface-roughness index (DSI) values. This value is affected by both the aggregation behavior and the surface roughness. The DSI values clearly suggest that the maltose particles had a tendency to aggregate, and it was not improved by the addition

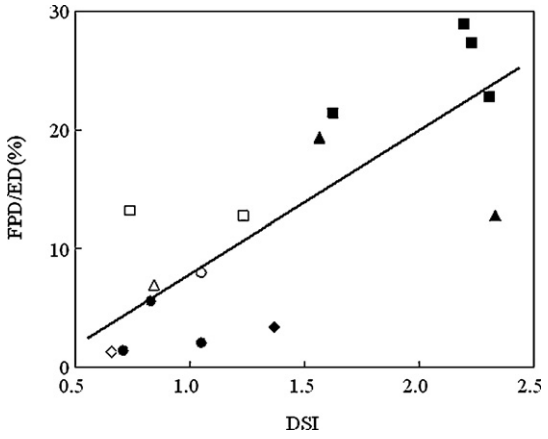

Fig. 9. Relationship between FPD/ED and DSI. (○) Mannitol, (□) mannitol/BSA, (△) mannitol/MC, (◊) mannitol/PVP, (●) maltose/BSA/Gelucire, (■) maltose/BSA, (▲) maltose/MC, and (♦) maltose/PVP.

of Tw80 or TPGS. The values much lower than unity could not be explained only by consumption of the adsorption site due to aggregation, but can be explained by the existence of enclosed particles in the aggregates that have no access to the external phase. It was significantly improved by the addition of Gelucire or SDS, although in the case of SDS, particle bursting should contribute to the increase in the surface area as well. When Gelucire was added, the DSI value slightly exceeded unity as well, meaning that surface roughness contributed to the increase in the DSI value, in addition to increased dispersity. Although the differentiation of the individual contribution of dispersity and the surface roughness was not possible in this analysis, the addition of Gelucire or SDS most likely improved dispersity.

3.7. Physical modification of the particle surface

In addition to the chemical modification of the particle surface using surfactant molecules, physical modification was attempted. This was done by adding polymer molecules. Fig. 8 shows SEM images when BSA or MC was added to maltose or lactose. It is clearly seen that the surface morphology became rough by the addition of polymer molecules. The most likely assumption for the formation of this structure is that the polymer film might be formed on surface of the droplets in the drying process first, followed by the rapid removal of the solvent inside to form wrinkles in the polymer films (Chang and Franses, 1995). The addition of a trace amount of the surfactant smoothed the surface structure, suggesting that the accumulation of surfactant molecules on the surface preferentially occurs over accumulation of the polymer molecules, which was a result of their slow diffusion. A direct interaction between the surfactants and the polymer molecules may be another reason for this observation, although no clear indication was found in Infrared and Circular Dichroism analysis (data not shown). Also observed was that the roughness decreased by replacing maltose with lactose. This might be due to crystallization of the lactose particles, because it causes extensive rearrangement of the molecules in the drying stage.

Although it was impossible to apply a cascade impactor investigation for maltose particles without carriers due to its sticky characteristics, these wrinkled particles could be evaluated because of their good dispersity even in the absence of the carrier. Fig. 9 shows a fraction of the fine particle dose (FPD), which was divided by the emitted dose (ED), as a function of DSI. Although the aerodynamic particle diameter varies from 3.9 to 7.4 μm in this dataset, a good correlation was found between these parameters, suggesting that surface roughness plays a dominant role in determining dispersity. This is in good agreement with the observation made by Adi et al. (2008), in which the surface roughness was determined by statistical analysis of the atomic force microscopy data. Therefore, in addition to the chemical modification of the particle surface, physical modification also seemed to be an important factor to be considered to improve the particle dispersity. This surface fabrication technique may become one of the key technologies to achieve an efficient pulmonary drug delivery system.

4. Conclusions

Control of the size and surface characteristics of spray-dried particles using an excipients approach was performed by understanding the dynamic process during spray-drying. The surface tension at 10 ms was found to correlate with both the size of the droplet produced from the spray nozzle and that of the particles after drying. Surfactant molecules accumulated spontaneously on the particle surface to improve surface characteristics including dispersity and hygroscopicity. Hollow particles were obtained using SDS as an additive. Moreover, the addition of polymer molecules was found to create a rough surface to improve the dispersity of the particles. Thus, the excipient approach seems to be a promising method to prepare fine drug particles of high dispersity for achieving an efficient pulmonary drug delivery.

Acknowledgments

The authors thank Kratos Analytical for performing XPS measurements. Also acknowledged is Nikkiso Co. for helping with droplet size measurements. High-speed video camera observations were made with the aid of Shimadzu Co. This work was in part supported by World Premier International Research Center (WPI) Initiative on Materials Nanoarchitectonics, MEXT, Japan.

References

Adi, H., Larson, I., Stewart, P.J., 2007. Adhesion and redistribution of salmeterol xinafoate particles in sugar-based mixtures for inhalation. Int. J. Pharm. 337, 229–238.
Adi, S., Adi, H., Tang, P., Traini, D., Chan, H.K., Young, P.M., 2008. Micro-particle corrugation, adhesion and inhalation aerosol efficiency. Eur. J. Pharm. Sci. 35, 12–18.
Bisgaard, H., Callaghan, C.O'., Smaldone, G.C., 2001. Drug Delivery to the Lung. Informa Healthcare, New York.
Chang, C.H., Franses, E.I., 1995. Adsorption dynamics of surfactants at the air/water interface: a critical review of mathematical models, data, and mechanisms. Colloids Surf. A 100, 1–45.
Chew, N.Y.K., Tang, P., Chan, H.K., Raper, J.A., 2005. How much particle surface corrugation is sufficient to improve aerosol performance of powders? Pharm. Res. 22, 148–152.
Chow, A.H.L., Tong, H.H.Y., Chattopadhyay, P., Shekunov, B.Y., 2007. Particle engineering for pulmonary drug delivery. Pharm. Res. 24, 411–437.
Edwards, D.A., Hanes, J., Caponetti, G., Hrkach, J., Ben-Jebria, A., Eskew, M.L., Mintzes, J., Deaver, D., Lotan, N., Langer, R., 1997. Large porous particles for pulmonary drug delivery. Science 276, 1868–1871.
Glover, W., Chan, H.K., Eberl, S., Daviskas, E., Verschuer, J., 2008. Effect of particle size of dry powder mannitol on the lung deposition in healthy volunteers. Int. J. Pharm. 349, 314–322.
Hadinoto, K., Phanapavudhikul, P., Kewu, Z., Tan, R.B.H., 2007. Dry powder aerosol delivery of large hollow nanoparticulate aggregates as prospective carriers of nanoparticulate drugs: effects of phospholipids. Int. J. Pharm. 333, 187–198.
Hickey, A.J., 2006. Inhalation Aerosols, 2nd edition. Informa Healthcare, New York.
Jones, M.D., Price, R., 2006. The influence of fine excipient particles on the performance of carrier-based dry powder inhalation formulations. Pharm. Res. 23, 1665–1674.
Jones, M.D., Hooton, J.C., Dawson, M.L., Ferrie, A.R., Price, R., 2008. An investigation into the dispersion mechanisms of ternary dry powder inhaler formulations by the quantification of interparticulate forces. Pharm. Res. 25, 337–348.
Katz, I.M., Schroeter, J.D., Martonen, T.B., 2001. Factor affecting the deposition of aerosolized insulin. Diabetes Technol. Ther. 3, 387–397.

Kawakami, K., Miyoshi, K., Ida, Y., 2004. Solubilization behavior of poorly soluble drugs with combined use of Gelucire 44/14 and cosolvent. J. Pharm. Sci. 93, 1471–1479.
Kawakami, K., Oda, N., Miyoshi, K., Funaki, T., Ida, Y., 2006. Solubilization behavior of a poorly soluble drug under combined use of surfactants and cosolvents. Eur. J. Pharm. Sci. 28, 7–14.
Okuyama, K., Lenggoro, I.W., 2003. Preparation of nanoparticles via spray route. Chem. Eng. Sci. 58, 537–547.
Park, S.S., Wexler, A.S., 2008. Size-dependent deposition of particles in the human lung at steady-state breathing. J. Aerosol Sci. 39, 266–276.
Patton, J.S., Byron, P.R., 2007. Inhaling medicines: delivering drugs to the body through the lungs. Nat. Rev. Drug Discov. 6, 67–74.
Priev, A., Zalipsky, S., Cohen, R., Barenholz, Y., 2002. Determination of critical micelle concentration of lipopolymers and other amphiphiles: comparison of sound velocity and fluorescent measurements. Langmuir 18, 612–617.
Shekunov, B.Y., Chattopadhyay, P., Tong, H.H.Y., Chow, A.H.L., 2007. Particle size analysis in pharmaceutics: principles, methods and applications. Pharm. Res. 24, 203–227.
Smith, H., 1994. ICRP Publication 66: Human Respiratory Tract Model for Radiological Protection. Pergamon, New York.
Tsapis, N., Burnnett, D., Jackson, B., Weitz, D.A., Edwards, D.A., 2002. Trojan particles: large porous carriers of nanoparticles for drug delivery. Proc. Natl. Acad. Sci. U.S.A. 99, 12001–12005.
Tong, H.H.Y., Shekunov, B.Y., York, P., Chow, A.H.L., 2006. Predicting the aerosol performance of dry powder inhalation formulations by interparticulate interaction analysis using inverse gas chromatography. J. Pharm. Sci. 95, 228–233.
Vehring, R., 2007. Pharmaceutical particle engineering via spray drying. Pharm. Res. 25, 999–1022.
Vehring, R., Foss, W.R., Lechuga-Ballesteros, D., 2007. Particle formation in spray drying. J. Aerosol Sci. 38, 728–746.
Wu, W.T., Yang, Y.M., Maa, J.R., 1998. Nucleate pool boiling enhancement by means of surfactant additives. Exp. Therm. Fluid. Sci. 18, 195–209.
Yang, W., Peters, J.I., Williams III, R.O., 2008. Inhaled nanoparticles—a current review. Int. J. Pharm. 356, 239–247.
Yang, Y., Bajaj, N., Xu, P., Ohn, K., Tsifansky, M.D., Yeo, Y., 2009. Development of highly porous large PLGA microparticles for pulmonary drug delivery. Biomaterials 30, 1947–1953.
Zeng, X.M., Martin, G.P., Tee, S.K., Marriott, C., 1998. The role of fine particle lactose on the dispersion and deaggregation of salbutamol sulfate in an air stream in vitro. Int. J. Pharm. 176, 99–110.
Zhang, J.T., Wang, B.X., 2003. Study on the interfacial evaporation of aqueous solution of SDS surfactant self-assembly monolayer. Int. J. Heat Mass Trans. 46, 5059–5064.